

# Structural Changes during ATP Hydrolysis Activity of the ATP Synthase from *Escherichia coli* as Revealed by Fluorescent Probes

Paola Turina<sup>1</sup>

F<sub>1</sub>F<sub>0</sub>-ATPase complexes undergo several changes in their tertiary and quaternary structure during their functioning. As a possible way to detect some of these different conformations during their activity, an environment-sensitive fluorescence probe was bound to cysteine residues, introduced by site-directed mutagenesis, in the  $\gamma$  subunit of the *Escherichia coli* enzyme. Fluorescence changes and ATP hydrolysis rates were compared under various conditions in F<sub>1</sub> and in reconstituted F<sub>1</sub>F<sub>0</sub>. The results are discussed in terms of possible modes of operation of the ATP synthases.

**KEY WORDS:** ATP synthase; *E. coli*; fluorescence; conformational changes; membrane energization.

## INTRODUCTION

F<sub>1</sub>F<sub>0</sub>-ATPases have been proved to be highly dynamic enzymes. Since the remarkable experiment by Noji *et al.* (1997), there is general acceptance in the field that ATP drives the rotation of the  $\gamma$  subunit with respect to the  $\alpha_3\beta_3$  barrel. The  $\epsilon$  subunit should move in concert with  $\gamma$ , as directly visualized in F<sub>1</sub> (Kato-Yamada *et al.*, 1998) and deduced in F<sub>1</sub>F<sub>0</sub> (Bulygin *et al.*, 1998; Aggeler *et al.*, 1997). That the rotational movement is transmitted to the *c* subunit ring, as a whole, is expected and has been visualized as well (Sambongi *et al.*, 1999; Pänke *et al.*, 2000), although its functional role in coupling still remains to be proved conclusively (Tsunoda *et al.*, 2000). Meanwhile, NMR studies have shown large structural rearrangements within the *c* monomer on protonation of its Asp61, which could determine the *c*-ring rotation with respect to the *a* subunit (Rastogi and Girving, 1999).

In addition, the  $\gamma$  and  $\epsilon$  subunits have been shown to undergo conformational changes also within themselves and possibly relative to each other upon nucleotide binding (reviewed in Capaldi *et al.*, 1996; Capaldi and Schulenberg, 2000) and upon membrane energization (reviewed in Richter and Gao, 1996). The need for an elastic coupling between F<sub>0</sub> and F<sub>1</sub> involving the  $\gamma/\epsilon$  and the *b*/ $\delta$  subunits has been pointed out (Cherepanov *et al.*, 1999; Oster and Wang, 2000). A complete picture of all the protein movements required for chemiosmotic coupling within the ATP synthase is far from being defined.

In parallel to the catalytic machinery, a different kind of machinery has yet to be at work in bringing about the inactive-to-active transition known to occur in photosynthetic and mitochondrial ATP synthases upon membrane energization. Recently, such  $\Delta\bar{\mu}_{H^+}$  activation has also been observed for the *E. coli* enzyme (Fischer *et al.*, 2000), suggesting it to be a general feature of all ATP synthases. The hydrolytic activity of the *E. coli* ATP synthase (EF<sub>1</sub>F<sub>0</sub>) was inhibited by ADP and P<sub>i</sub> and activated by  $\Delta\bar{\mu}_{H^+}$  and possibly by ATP (Fischer *et al.*, 2000).

One approach, among several applied to detect and localize movements within the ATP synthase, has

<sup>1</sup> Laboratory of Biochemistry and Biophysics, Department of Biology, University of Bologna, Via Irnerio 42, I-40126 Bologna, Italy. e-mail: turina@alma.unibo.it

been the use of environment-sensitive fluorescent probes covalently attached to specific subunits. This chapter will focus on data obtained using this approach and on their interpretation.

### THE $\gamma$ SUBUNIT CONFORMATION REARRANGES UPON ATP BINDING AND ATP BOND CLEAVAGE

The fluorescent probe coumarin maleimide (CM) was covalently bound at different positions in the  $\gamma$  subunit via site-directed cysteine residues. At two of these positions ( $\gamma$ 106 and  $\gamma$ 8), changes in the steady-state fluorescence of the probe could be detected in  $EF_1$  upon binding of ATP and its noncleavable analog AMP-PNP, but not upon binding of ADP (Turina and Capaldi, 1994a). Titration with AMP-PNP of the signal of CM bound at  $\gamma$ 106 indicated that the maximal fluorescence change occurred with the binding of 1 mole of AMP-PNP per mole  $EF_1$  at the high-affinity site. Under conditions of unisite hydrolysis, the fluorescence of CM at  $\gamma$ 106 was shown to increase with the same kinetics of ATP binding to the high-affinity catalytic site and to decrease back to the original level with the same kinetics of catalytic events. Similar fluorescence traces could be obtained repeatedly by subsequent additions of similar amounts of ATP, as would be expected if the conformation of the enzyme returned each time back to the initial one. The catalytic step kinetically associated with the fluorescence decrease was then shown to be the cleavage of ATP (Turina and Capaldi, 1994b). Figure 1A shows the time course of fluorescence changes after the start of unisite hydrolysis of ATP. The data were analyzed based on a kinetic model for the unisite catalysis (Grubmeyer *et al.*, 1982) using kinetic constant values, which could describe the kinetics of unisite ATP hydrolysis catalyzed by CM-labeled  $\gamma$ T106C- $EF_1$ . In addition, the maximum fluorescence enhancement obtained with AMP-PNP was correlated with full occupancy of the high-affinity catalytic site. The solid line represents the fraction of enzyme expected to be in the  $F_1 \cdot \text{ATP}$  state, while the fraction of enzyme expected to be both in the  $F_1 \cdot \text{ATP}$  and the  $F_1 \cdot \text{ADP} \cdot \text{P}_i$  states is indicated by the dashed line.

As an additional proof that the increased fluorescence of CM was due to the  $F_1 \cdot \text{ATP}$  state only, fluorescence signals were measured also with the analog ATP $\gamma$ S. In several ATPases, the ATP $\gamma$ S is hydrolyzed more slowly than ATP or not at all because of the

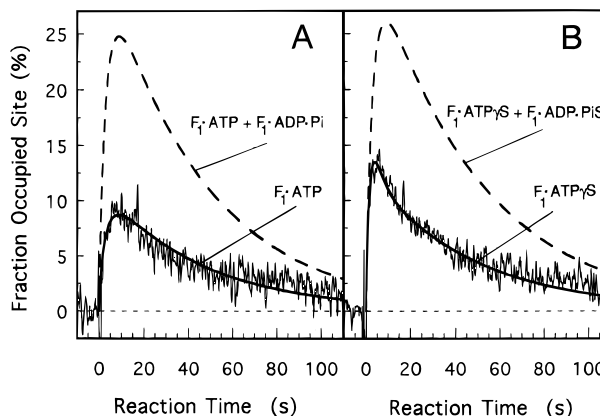
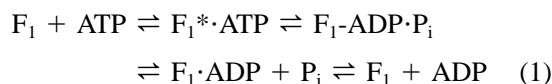


**Fig. 1.** Fluorescence changes induced by ATP and ATP $\gamma$ S unisite hydrolysis in CM-labeled  $\gamma$ T106C- $EF_1$ . The fluorescence emission was recorded at 430 nm upon excitation at 395 nm. The enzyme concentration was 1  $\mu$ M and the concentration of the nucleotide, added at time  $t = 0$ , was 305 nM. The solid lines represent the enzyme fraction expected to be in the  $F_1 \cdot \text{ATP}$  (A) or  $F_1 \cdot \text{ATP}\gamma\text{S}$  (B) state according to the unisite kinetic model and rate constants reported in Turina and Capaldi (1994b). The dashed lines represent the enzyme fraction expected to be in both states  $F_1 \cdot \text{ATP}$  and  $F_1 \cdot \text{ADP} \cdot \text{P}_i$  (A) or  $F_1 \cdot \text{ATP}\gamma\text{S}$  and  $F_1 \cdot \text{ADP} \cdot \text{P}_i\text{S}$  (B) according to the same kinetic mechanism. Reproduced from Turina and Capaldi (1994b) with minor modifications.

lower reactivity of the  $\gamma$ -phosphorothioate group toward nucleophilic attack (Eckstein, 1983). Consistently, the time course of [ $^{35}\text{S}$ ]P $_i$ S release catalyzed by CM-labeled  $\gamma$ T106C- $EF_1$  under unisite conditions showed a lag, well fitted by kinetic constants values for ATP $\gamma$ S cleavage and formation, which were 30-fold lower with respect to the corresponding kinetic constants for ATP. During this lag, not present in the time course of [ $^{32}\text{P}$ ]P $_i$  release, an initial accumulation of uncleaved ATP $\gamma$ S on the enzyme, not in equilibrium with its hydrolysis products, was expected, i.e., a concentration of the  $F_1 \cdot \text{ATP}\gamma\text{S}$  complex initially higher than the corresponding  $F_1 \cdot \text{ATP}$  concentration. On the contrary, the sum of the two complexes  $F_1 \cdot \text{ATP}\gamma\text{S} + F_1 \cdot \text{ADP} \cdot \text{P}_i\text{S}$  was predicted to be practically indistinguishable from the corresponding  $F_1 \cdot \text{ATP} + F_1 \cdot \text{ADP} \cdot \text{P}_i$  sum over the entire time course. As expected, the time course of fluorescence changes at  $\gamma$ 106, triggered by unisite amounts of ATP $\gamma$ S, showed this initial accumulation (see Fig. 1B), confirming that the higher fluorescence state was lost on the  $F_1 \cdot \text{ATP}\gamma\text{S} \rightarrow F_1 \cdot \text{ADP} \cdot \text{P}_i\text{S}$  transition (cleavage), rather than on the  $F_1 \cdot \text{ADP} \cdot \text{P}_i\text{S} \rightarrow F_1 \cdot \text{ADP} + \text{P}_i\text{S}$  transition (P $_i$ S release from the enzyme).

The higher fluorescence of the CM bound at  $\gamma$ 106 associated with the species  $F_1 \cdot \text{ATP}$  can be interpreted

as being due to a different conformation of the protein in this state. Therefore, a minimal scheme based on these data is the following:



with  $F_1^*$  indicating the different conformational state.

In particular, the data obtained with ATP $\gamma$ S indicate that the  $F_1^* \rightarrow F_1$  transition does not occur before ATP cleavage. Instead, it occurs as a result of transition state formation, either in concert with it or later, when the  $\gamma$ - $\beta$  phosphate bond is already broken, but the  $P_i$  has not been yet released from the enzyme. In this respect, it is interesting to consider what is already known about the S1 fragment of *Dictyostelium* myosin, for which X-ray structures have been resolved for the MgADP·BeF<sub>3</sub>·S1 complex (Fischer *et al.*, 1995) and for the MgADP·VO<sub>4</sub>·S1 complex (Smith and Rayment, 1996). These two structures are considered to reflect the MgATP·S1 complex and the S1 in complex with the bipyramidal transition state, respectively. An extended series of residues exhibits different conformations in the beryllium and vanadate complexes, including the 25 kDa COOH-terminal section of the heavy chain, which in the vanadate complex has translated 23 Å and rotated approximately 70° relative to the position in the beryllium complex. This change affects residues, which are up to 50 Å away from the ATP binding site, without affecting the residues in the ATP binding site itself. Similarly, in the case of EF<sub>1</sub>, the  $\gamma$ 106 residue lies at least 60 Å away from the catalytic sites (Hausrath *et al.* 1999) and has no direct van der Waals contacts with the  $\alpha/\beta$  subunits. Therefore, the fluorescence changes observed for the CM bound at  $\gamma$ 106 are the results of long-range transmission of movement from the catalytic site to the  $\gamma$  subunit, in a domain of this subunit, which points toward F<sub>0</sub>.

Interestingly, the transmission of such movement seems to require the mediation of the  $\epsilon$  subunit. In  $\epsilon$ -depleted EF<sub>1</sub> complexes, the ATP hydrolysis-driven fluorescence changes at both the  $\gamma$ 106 and the  $\gamma$ 8 were lost (Turina and Capaldi, 1994a), a result that parallels the loss of nucleotide-induced conformational changes upon  $\epsilon$  removal, as detected by crosslinking (Aggeler and Capaldi, 1993) and electron microscopy image analysis (Wilkins and Capaldi, 1994). It is possible that, in the whole EF<sub>1</sub>, the CM bound at  $\gamma$ 106 is in contact with the  $\epsilon$  subunit, and therefore, it could be considered that the changes in the physicochemical

environment experienced by the CM were due to the rearranging  $\gamma/\epsilon$  contacts. However, the ATP hydrolysis-induced fluorescence changes were also lost when the CM was bound at the  $\gamma$ 8 residue, which lies close to the catalytic sites fully surrounded by the  $\alpha_3\beta_3$  barrel, where it cannot make direct contacts with the  $\epsilon$  subunit. Therefore, it seems much more likely that the  $\gamma$  subunit rearrangements detected by these studies occur because the  $\epsilon$  subunit acts as a primary transmission element between the events at the high-affinity catalytic site in the  $\beta$  subunit and the  $\gamma$  subunit. Evidence of movements of  $\epsilon$  and within  $\epsilon$ , depending on which nucleotide is in the catalytic site, are plentiful and have been extensively reviewed (Capaldi *et al.*, 1996; Capaldi and Schulenberg, 2000).

The central question about the conformational changes detected by these studies is to understand their role in the ATP synthase functioning. Since they have been shown to depend on the presence of  $\epsilon$ , while the ATP-driven rotation of  $\gamma$  can take place in the absence of this subunit, it seems reasonable to exclude that they are directly linked to the rotation of  $\gamma$ . Moreover, evidence has been presented that unisite catalysis does not drive rotation (Garcia and Capaldi, 1998; Tsunoda *et al.* 1999). As it has been widely recognized (Jencks, 1980; Zhou and Boyer, 1993; Cross, 2000; Boyer, 2000), an efficient functioning of the ATP synthase may need the ability of its machinery to distinguish between the F<sub>1</sub>F<sub>0</sub>·ATP and the F<sub>1</sub>F<sub>0</sub>·ADP·P<sub>i</sub> state, such that, during synthesis, ATP is released, as opposed to ADP and P<sub>i</sub>, and energy is not wasted. Whether the ATP in the catalytic site has been cleaved or has been synthesized, needs to be signaled to the proton translocation pathway in F<sub>0</sub>. The movements of  $\gamma$  detected by the CM fluorescence could coincide with this signaling. During synthesis, the 120° rotation, with the associated ATP release, might not occur unless the  $\epsilon$  and  $\gamma$  subunits have rearranged to the appropriate conformation. In this case, the  $\gamma/\epsilon$  conformation of F<sub>1</sub><sup>\*</sup>, induced by ATP, would be the one allowing the actual rotation to take place, while the  $\gamma/\epsilon$  conformation in the presence of ADP and P<sub>i</sub> would only allow the resting position. This conformational switch would then be part of a “coupling control,” which does not allow rotation (and, hence, H<sup>+</sup> translocation) to occur in the synthesis direction unless ATP has been formed in the catalytic site.

One more point deserves to be taken into consideration. The unisite catalysis is usually considered to be a partial reaction of the “normal” multisite catalysis. This general view is supported by data indicating that

unisite catalysis is accelerated to fast rates by multiple sites nucleotide binding, both in hydrolysis and in synthesis (Cross *et al.*, 1982; Penefsky, 1985a), and that unisite release of [ $^{14}\text{C}$ ]ATP can take place from medium  $\text{P}_i$  and medium unisite [ $^{14}\text{C}$ ]ADP in the presence of a proton gradient (reviewed in Gräber and Labahn, 1992). However, the possibility exists that the unisite catalysis represents a sort of “starter,” after which multisite, multiple turnover rotational catalysis is allowed to proceed. Data from several laboratories appear to be consistent with the view of heterogeneous catalytic pathways for unisite and multisite modes of operation (Bullough *et al.*, 1987; Fromme and Gräber, 1989; Zhang and Jagendorf, 1995; Possmayer *et al.*, 2000). The recent evidence indicating lack of rotation during unisite catalysis (Garcia and Capaldi, 1998; Tsunoda *et al.*, 1999) add support to this view. Such a “starter” step could well coincide with a rearrangement of the rotor, such as to make its rotation possible. If this was the case, then the conformational changes of the  $\gamma$  subunit detected by CM could represent this sort of “priming” or “activation” of the ATP synthase antecedent to the actual multisite cycling. Although this possibility has not been widely discussed until now, it cannot be completely ruled out.

### REARRANGEMENTS OF $\gamma$ SUBUNIT IN THE RECONSTITUTED $\text{EF}_1\text{F}_0$

With the aim of studying the CM fluorescence also in the whole  $\text{EF}_1\text{F}_0$ , liposomes containing wild-type enzyme were stripped of  $\text{F}_1$  and CM-labeled  $\gamma\text{T106C-EF}_1$  was rebound in its place. The vesicles with incorporated CM-labeled  $\text{EF}_1\text{F}_0$  were relatively well coupled, in that they were able of ATP-induced proton pumping as measured by the ACMA quenching and of acid–base-driven ATP synthesis (with an ATP synthesis rate of about  $10 \text{ ATP} \cdot (\text{EF}_1\text{F}_0 \cdot \text{s})^{-1}$ ). Parallel samples in which wild-type  $\text{EF}_1$  or unlabeled  $\gamma\text{T106C-EF}_1$  were rebound yielded quantitatively similar results. An aliquot of the CM-labeled  $\text{EF}_1\text{F}_0$  vesicles was treated with dicyclohexylcarbodiimide (DCCD) until about 7% of the original ATPase activity was left. The activity of these DCCD-derivatized samples, treated with the detergent lauryldimethylamine oxide (LDAO), which functionally uncouples  $\text{F}_1$  from  $\text{F}_0$ , was 97% of the original, indicating that the DCCD was predominantly bound to  $\text{F}_0$ .

The signals obtained after addition of multisite concentrations of AMP–PNP and ATP to these CM-

labeled vesicles were qualitatively the same as those obtained with  $\text{EF}_1$ , with AMP–PNP, causing a stable enhancement of the fluorescence signal and ATP, an enhancement approximately 30% of the one induced by AMP–PNP, followed by a decay (in the presence of uncouplers, see below).

Because of the high light-scattering of the proteoliposomes suspension, it was not possible to detect ATP-induced fluorescence changes with substoichiometric  $\text{ATP}:\text{EF}_1\text{F}_0$  ratios. Figure 2, trace –DCCD, shows the signal, uncorrected for light scattering, obtained by adding amounts of ATP stoichiometric with  $\text{EF}_1\text{F}_0$ . Under these conditions, it is expected that a small percentage of the enzyme will bind at more than one site, but most of the signal will still come from enzyme, which has bound only one ATP. As seen for  $\text{EF}_1$ , an initial increase in fluorescence was followed by a decrease, with a time course similar to the ones obtained for  $\text{EF}_1$  under unisite conditions (compare Fig. 1). By analogy with  $\text{EF}_1$ , the initial increase can be attributed to ATP binding, and the following decrease can be attributed to ATP cleavage into ADP and  $\text{P}_i$ . Interestingly, when the same stoichiometric addition of ATP was made to the DCCD-inhibited proteoliposomes, a similar fluorescence enhancement was observed initially, while the following decrease was significantly slowed down (Fig. 2, trace + DCCD). This indicates that the catalytic ATP cleavage is either blocked or significantly slowed down when the cAsp61 is derivatized with DCCD, which, in turn, implies that the conformational change detected by the CM fluorescence is normally transmitted down to cAsp61.

On the whole, these data are consistent with those obtained by Matsuno-Yagi and Hatefi (1993), who measured the time course of unisite ATP bound to the mitochondrial  $\text{F}_1\text{F}_0$  and found that DCCD derivatization would significantly increase the permanence of uncleaved ATP on the enzyme. As already noted by these authors, this behavior is in contrast to what was reported by Penefsky (1985b), who measured instead, in the DCCD-derivatized mitochondrial  $\text{F}_1\text{F}_0$ , a blockage of unisite ATP binding.

A similar, apparently contradictory behavior of the DCCD-treated enzyme has also been found for  $\text{EF}_1\text{F}_0$ . Mendel-Hartvig and Capaldi (1991) showed that the conformation of the  $\epsilon$  subunit, as monitored by trypsin digestion and  $\beta$ - $\epsilon$  crosslink, was different according to which nucleotides were present during the DCCD derivatization, whereas it was independent of the nucleotides present during trypsinization or

crosslink, once the DCCD was bound. These authors concluded that DCCD blocked the nucleotide-induced conformational changes, freezing the enzyme in the one or the other conformation. The data presented in Fig. 2 indicate that, once the nucleotide has bound to the DCCD-derivatized  $EF_1F_0$ , the conformational change blocked is the one linked to unisite ATP cleavage and detected by the fluorescence decrease of CM bound at  $\gamma 106$ .

In addition, the data of Fig. 2 suggest that the conformational transition on ATP binding is not the reversal of the conformational transition on ATP cleavage, since it is difficult to imagine how DCCD would cause a sort of one-way inhibition. Therefore, it is most likely that during unisite catalysis, the enzyme experiences at least a third conformation, which, however, is not detected by CM bound at  $\gamma 106$ .

### MEDIUM ADP AND $P_i$ CAN DESTABILIZE THE ATP-INDUCED CONFORMATION

In  $EF_1$ , the non-cleavable analog AMP-PNP caused a fluorescence enhancement up to 75% (at 430 nm), which did not reverse. With multisite concentrations of ATP, the fluorescence of CM bound at  $\gamma 106$  would rapidly increase and then slowly decrease again, unless an ATP-regenerating system (phosphoenolpyruvate + pyruvate kinase) was present, in which case no decrease was observed up to 10 min (Turina and

Capaldi, 1994a). Similarly with ATP $\gamma$ S, although in this case the maximum fluorescence increase observed prior to the decrease was about twice as high as with ATP and similar to the fluorescence increase observed with saturating amount of AMP-PNP. The three nucleotides caused the same shift of the emission spectrum of CM, indicating that the conformational rearrangement induced by each of them is probably the same and that the lower steady-state level of fluorescence increase observed with ATP was due to rapid cleavage of ATP and, therefore, to a lower enzyme fraction in the  $F_1 \cdot$ ATP state.

Comparison of the data obtained with AMP-PNP, ATP/ATP $\gamma$ S, and ATP in the presence of a regenerating system, allowed the hypothesis that the slow reversal of fluorescence enhancement observed with both cleavable nucleotides could be ascribed to ADP and  $P_i$  (or  $P_i$ S) production. In support of this hypothesis, the addition of ADP or  $P_i$  during the ATP-induced fluorescence enhancement would strongly accelerate the fluorescence decrease (Fig. 3A and B). Similar effects were observed in  $EF_1F_0$  (in the presence of uncouplers, see below). For both  $EF_1$  and  $EF_1F_0$ , addition of increasing concentrations of  $P_i$  together with ATP would inhibit the extent of the ATP-induced fluorescence enhancement with an half-maximal effect at 276  $\mu$ M (see Fig. 3C). It should be noted that this effect of  $P_i$  probably required ADP, present in trace amounts in the ATP, since in the presence of pyruvate kinase and phosphoenolpyruvate the ATP-induced fluorescence increase was stable for periods of time long enough to generate substantial amounts of  $P_i$  in the cuvette. For  $EF_1$ , the [ $\gamma$ - $^{32}$ P]ATP hydrolysis activity was measured under conditions identical to those of the fluorescence assay and an inhibition of this activity was found with increasing  $P_i$ , with the same concentration dependence as found for inhibition of ATP-induced fluorescence enhancement (Fig. 3C). Notice that high  $P_i$  concentrations did not saturate either fluorescence quenching or activity inhibition, possibly due to the low ADP concentrations in these assays.

These data indicate that ADP and  $P_i$  can bind to the enzyme, thereby destabilizing the ATP-induced conformation and causing the transition to a different conformation, which is inhibited. It can only be speculated whether this ADP/ $P_i$ -induced fluorescence decrease is associated to the  $F_1^* \cdot \text{ATP} \rightarrow F_1 \cdot \text{ADP} \cdot P_i$  conversion at the high-affinity catalytic site, to an affinity change, which releases ATP (i.e.,  $F_1^* \cdot \text{ATP} \rightarrow F_1 + \text{ATP}$ ), or to the different nucleotide binding pattern:  $F_1^* \cdot \text{ATP} + \text{ADP} + P_i \rightarrow \text{ADP} \cdot P_i F_1 \cdot \text{ATP}$ . It has

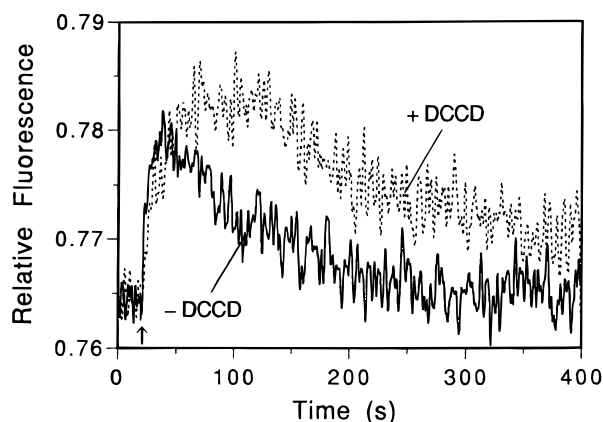


**Fig. 2.** Fluorescence changes induced by ATP hydrolysis catalyzed by CM-labeled  $\gamma$ T106C- $EF_1F_0$  in the absence or in the presence of DCCD. The fluorescence emission was recorded at 430 nm. The enzyme concentration was 815 nM for both the untreated and the DCCD-treated enzyme. ADP was also present at a concentration of 800 nM (see Turina and Capaldi, 1994b). ATP was added at the time indicated by the arrow at a final concentration of 805 nM.

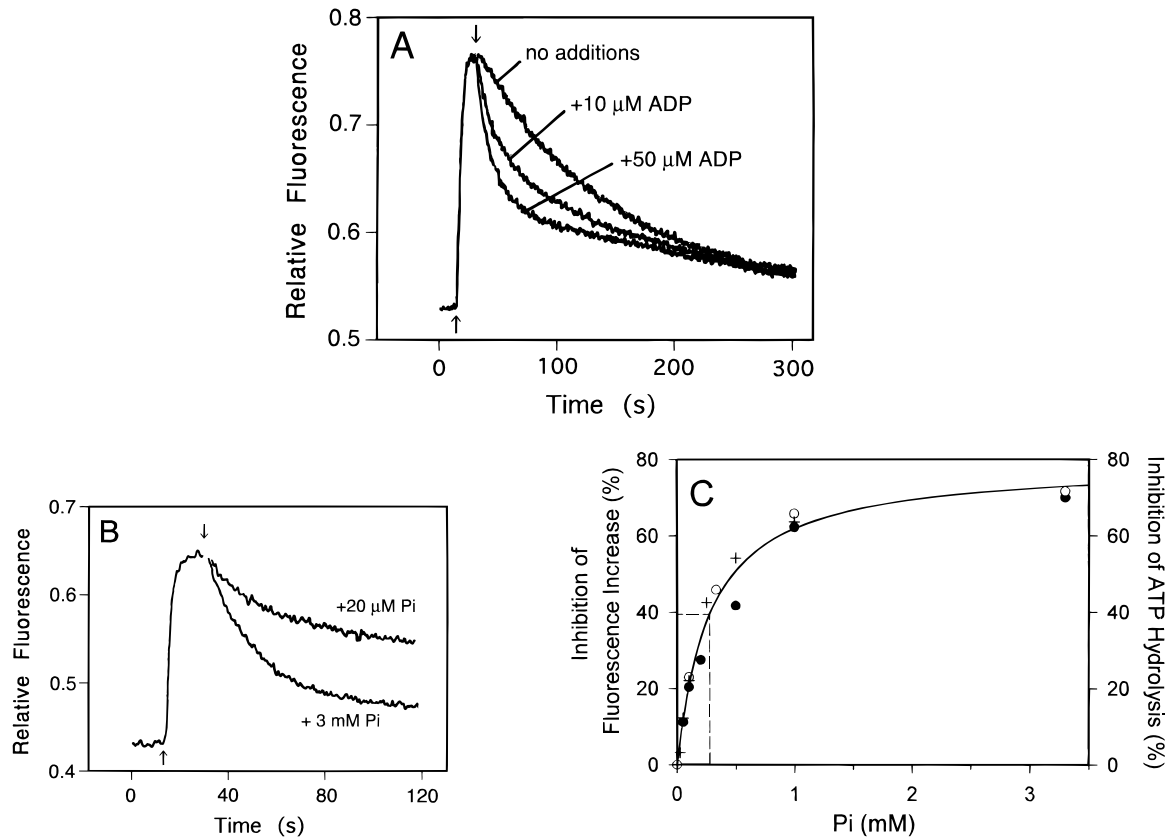
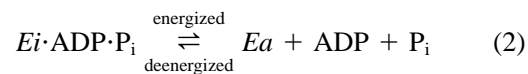


**Fig. 3.** Fluorescence changes induced by ATP, ADP, and  $P_i$  in CM-labeled  $\gamma$ T106C-EF<sub>1</sub> and  $\gamma$ T106C-EF<sub>1</sub>F<sub>0</sub>. The fluorescence emission was recorded at 430 nm. (A). The concentration of CM-labeled  $\gamma$ T106C-EF<sub>1</sub> was 100 nM. At the time indicated by the first arrow, ATP was added at a final concentration of 3  $\mu$ M. At the second arrow ADP was added at the indicated concentrations. (B). The concentration of CM-labeled  $\gamma$ T106C-EF<sub>1</sub> was 100 nM. At the time indicated by the first arrow, ATP was added at a final concentration of 100  $\mu$ M. At the second arrow  $P_i$  was added at the indicated concentrations. (C). The fluorescence increase upon addition of ATP together with increasing concentrations of  $P_i$  was recorded for CM-labeled  $\gamma$ T106C-EF<sub>1</sub> (●) and for CM-labeled  $\gamma$ T106C-EF<sub>1</sub>F<sub>0</sub> (○). The enzyme concentrations were 100 nM and 50 nM and the ATP concentrations 100  $\mu$ M and 1 mM, respectively. The 100% (0% inhibition) refers to the ATP-induced increase in the absence of added  $P_i$ . The initial rate of hydrolysis of 1 mM [ $\gamma$ -<sup>32</sup>P]ATP catalyzed by 0.5  $\mu$ M CM-labeled  $\gamma$ T106C-EF<sub>1</sub> (+) was measured at various concentrations of  $P_i$ , added together with the [ $\gamma$ -<sup>32</sup>P]ATP. The 100% (0% inhibition) refers to the hydrolysis rate in the absence of added  $P_i$ .

been shown that the binding of ADP and  $P_i$  to the mitochondrial  $F_1$  would cause the release of AMP-PNP which had been previously tightly bound (Nalin and Cross, 1982). It is not impossible that ADP and  $P_i$  binding to  $F_1$ \*-ATP and  $F_1F_0$ \*-ATP might cause both an accelerated cleavage and an increased release of ATP. A decreased affinity for ATP would also be consistent with the reduced ATP-hydrolysis activity of the form, which has bound medium ADP and  $P_i$ .

Recently, the binding of ADP and  $P_i$  to EF<sub>1</sub>F<sub>0</sub> was shown to inhibit its hydrolytic activity down to 2% (Fischer *et al.*, 2000). These authors have shown that a  $\Delta\mu_{H^+}$ -induced conformational change could reverse, at least in part, this inhibition, suggesting the following scheme:



where  $Ei$  and  $Ea$  indicate the inhibited and the active conformation, respectively. After collapsing the  $\Delta\mu_{H^+}$ , and in the presence of ADP and  $P_i$ , the  $Ea$  form was found to be unstable and to decay completely after approximately 100 turnovers. In the absence of ADP and  $P_i$ , the ATP hydrolysis was already high and no further activation by  $\Delta\mu_{H^+}$  was found.

By comparing these different sets of data, two main possibilities can be considered. It can be that the conformational changes of the  $\gamma$  subunit detected by CM depend on the state of the enzyme, i.e., if the enzyme is in the active state ( $Ea$ ), then the ATP can

bind and can induce the  $\gamma/\epsilon$  conformation characteristic of  $F_1^*$ . Conversely, it can be that the state of the enzyme (its active,  $Ea$ , or inhibited,  $Ei$ , state) depends on the conformational changes of the  $\gamma/\epsilon$  subunits, i.e., when ATP is bound to the high-affinity catalytic site and the  $\gamma/\epsilon$  conformation is changed, then the enzyme is transformed into the active state,  $Ea$ . In the first hypothesis, the high- and low-fluorescence forms could interconvert rapidly at each catalytic turnover, while the enzyme is in the  $Ea$  state, consistent with the possible “signaling” role of this  $\gamma$  rearrangement during catalytic cycling, as discussed above. On the contrary, the second hypothesis is consistent with the role of unisite ATP hydrolysis as a “priming” step, activating the enzyme.

#### MEMBRANE ENERGIZATION PREVENTS THE $\gamma$ REARRANGEMENT INDUCED BY ADP AND $P_i$ AT THE SAME TIME PREVENTING ENZYME INHIBITION

When the fluorescence of CM bound at  $\gamma 106$  in the  $EF_1F_0$  incorporated in liposomes was monitored upon addition of multisite concentrations of ATP, a different result was obtained, whether uncouplers were present to dissipate the ATP hydrolysis-induced  $\Delta\bar{\mu}_{H^+}$  or not (Fig. 4A). In the presence of uncouplers, the fluorescence signal increased upon addition of ATP and then slowly decreased again, as already observed for  $EF_1$ . Without uncouplers added, the higher fluorescence level induced by ATP was maintained for at least 10 min, similar to what was seen in the presence of an ATP-regenerating system. It could be argued that the effect of the ATP-induced  $\Delta\bar{\mu}_{H^+}$  was to inhibit ATP hydrolysis and the following ADP and  $P_i$  concentration increase. However, when the  $[\gamma\text{-}^{32}\text{P}]\text{-ATP}$  hydrolysis was measured in parallel samples, the amount of ATP hydrolyzed during these 10 min was very similar regardless of the presence of uncouplers (Fig. 4B). In both cases, the percentage of hydrolyzed ATP after 10 min was approximately 45%, i.e., the ADP and  $P_i$  concentrations in the assay were, in both cases, approximately 450  $\mu\text{M}$ . However, if the instant rates of hydrolysis with and without uncouplers are compared along the whole time course by plotting their ratio at each time point (inset), what becomes evident is a progressive differential inhibition of the uncoupled rate with respect to the coupled rate. In other words, both hydrolysis rates were progressively inhibited in time, probably due to substrate depletion and/or prod-

ucts formation, but the uncoupled hydrolysis was more inhibited than the coupled one. This additional inhibition can be attributed to ADP and  $P_i$  binding and concomitant conformational transition from the active to the inhibited form of the enzyme, as discussed above. The presence of an ATP-induced  $\Delta\bar{\mu}_{H^+}$  prevented both the fluorescence decrease and the enzyme inhibition (Fig. 4A and inset, B). An energized membrane appears to prevent the transition toward the inhibited form, in agreement with reaction (2).

In principle, an ATP-generated  $\Delta\bar{\mu}_{H^+}$  should also inhibit the enzyme because of its backpressure. An inhibition of up to five-fold has been observed in well-coupled  $EF_1F_0$  proteoliposomes (Fischer *et al.*, 2000). Since a steady-state  $\Delta\bar{\mu}_{H^+}$  is likely to become established within the first few seconds, during which the formation of inhibiting ADP/ $P_i$  is still negligible, the ratio of the uncoupled versus coupled ATP hydrolysis rates in this time range should be a good estimate of the inhibition due to the  $\Delta\bar{\mu}_{H^+}$  backpressure. In the inset of Fig. 4B it can be seen that this ratio is at the beginning slightly higher than 1 (1.5), indicating that the degree of  $EF_1F_0$  incorporation into these proteoliposomes was good enough to see some ATP synthesis induced by acid-base transitions and ATP-induced ACMA quenching, as mentioned above, but not as good as to have a strong inhibition of ATP hydrolysis.

The fluorescence of CM bound to  $\gamma 106\text{-}EF_1F_0$  upon addition of multisite concentrations of ATP with and without uncouplers was also monitored in the presence of 1 mM  $P_i$  (Fig. 4C). In both cases, the initial increase of fluorescence was lower than in the absence of  $P_i$ , as expected (compare Fig. 3C). The subsequent decrease of fluorescence observed in time in the absence of  $\Delta\bar{\mu}_{H^+}$  can be attributed mainly to an increase in the ADP concentration, since the  $P_i$  concentration was already high. In the presence of a  $\Delta\bar{\mu}_{H^+}$ , not only the fluorescence decrease was prevented as in the absence of added  $P_i$  compare (Fig. 4A, trace *no uncouplers*), but it increased steadily in time. After 20 min, the fluorescence increase had reached a value similar to the one observed initially in the absence of  $P_i$ .

Again, the time course of  $[\gamma\text{-}^{32}\text{P}]\text{ATP}$  hydrolysis measured in parallel samples did not differ significantly at a first sight (Fig. 4D), yet by taking the ratio of uncoupled versus coupled ATP hydrolysis rate over the time course (inset), it can be seen that the uncoupled rate is progressively more inhibited in time, with a decay similar to the decay of the fluorescence signal. As seen for the measurements in the absence of  $P_i$ , also in this case the initial rate of ATP hydrolysis was

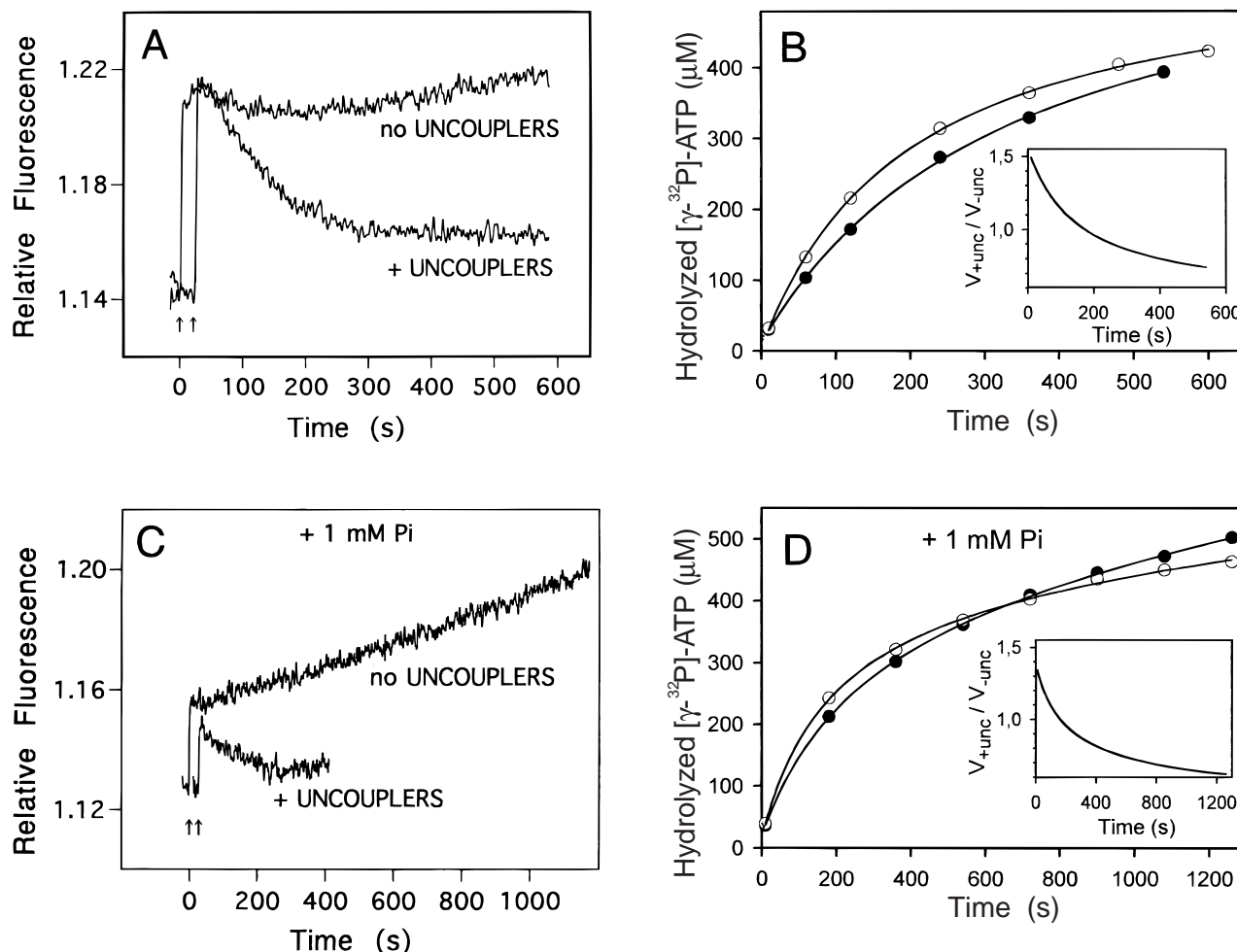


**Fig. 4.** ATP hydrolysis catalyzed by CM-labeled  $\gamma$ T106C- $\text{EF}_1\text{F}_0$  incorporated into liposomes in the presence or in the absence of uncouplers. The enzyme concentration was 50 nM. The ATP hydrolysis was started by the addition of 1 mM ATP (A and C) or 1 mM  $[\gamma\text{-}^{32}\text{P}]\text{ATP}$  (B and D).  $\text{P}_i$ , at a final concentration of 1 mM, was added together with ATP (C and D). The uncouplers were 1  $\mu\text{M}$  nigericin and valinomycin in the presence of 50 mM KCl. (A) and (C). The fluorescence emission was recorded at 430 nm. The arrows indicate ATP addition to proteoliposomes. Uncouplers were present as indicated. (B) and (D).  $[\gamma\text{-}^{32}\text{P}]\text{ATP}$  was added to proteoliposomes at the time  $t = 0$  in the presence (○) or in the absence (●) of uncouplers. The solid lines are best-fit of arbitrary functions to the experimental data. In the insets, the first derivative of the best-fit function in the presence of uncouplers ( $V_{+\text{unc}}$ ) divided by the first derivative of the best-fit function in the absence of uncouplers ( $V_{-\text{unc}}$ ) is reported.

slightly higher in the uncoupled sample, indicating inhibition due to  $\Delta\bar{\mu}_{\text{H}^+}$  backpressure. Again, the differential inhibition developed in time can be attributed to ADP and  $\text{P}_i$  binding, which induce the inhibited conformation of the enzyme. In the presence of an ATP-induced  $\Delta\bar{\mu}_{\text{H}^+}$ , the active-to-inactive transition is prevented and the reverse transition is favored, as seen from the observed fluorescence increase (trace *no uncouplers*, Fig. 4C), in agreement with reaction (2).

## CONCLUSION

With the use of the fluorescent probe CM covalently attached to the  $\gamma$  subunit of the *E. coli* ATP synthase, it has been shown that a conformational change of  $\gamma$  occurs upon binding of ATP to the high-affinity catalytic site and that a second conformational change occurs upon catalytic ATP cleavage. In the whole  $\text{EF}_1\text{F}_0$ , this second change is strongly inhibited



by DCCD bound to  $F_0$ . These conformational rearrangements depend on the presence of the  $\epsilon$  subunit and are not part of the rotational movements of the  $\gamma$  subunit.

It can be envisioned that these rearrangements take place for every turnover during the multisite activity of the enzyme or, as an alternative hypothesis, that they constitute a sort of priming of the enzyme, preparing it for high-speed rotation. During multisite ATP hydrolysis, the fraction of enzyme in the ATP-induced conformation, as revealed by fluorescence enhancement, is correlated to the fraction of enzyme in the  $\Delta\bar{\mu}_{H^+}$ -activated state. This correlation is consistent with both hypotheses. In the first case it indicates that the steady-state level of the  $F_1F_0^*\cdot\text{ATP}$  species occurring at each turnover is higher when the enzyme fraction in the  $\Delta\bar{\mu}_{H^+}$ -activated state is higher. In the second case the  $F_1F_0^*\cdot\text{ATP}$  conformation coincides with the activated state. This second possibility implies that the conformation induced by ATP binding in the high-affinity site coincides with the  $\Delta\bar{\mu}_{H^+}$ -induced conformation and that the catalytic events at the high-affinity site determine the transition to the activated state of the enzyme. At the moment there is uncertainty about this point, which hopefully some of the future work on the ATP synthase will address.

## REFERENCES

- Aggeler, R. and Capaldi, R. A. (1993). *J. Biol. Chem.* **268**, 14576–14578.
- Aggeler, R., Ogilvie, I., and Capaldi, R. A. (1997). *J. Biol. Chem.* **272**, 19621–19624.
- Boyer, P. D. (2000). *Biochim. Biophys. Acta* **1458**, 252–262.
- Bullough, D. A., Verburg, J. G., Yoshida, M., and Allison, W. S. (1987). *J. Biol. Chem.* **262**, 11675–11683.
- Bulygin, V. V., Duncan, T. M., and Cross, R. L. (1998). *J. Biol. Chem.* **273**, 31765–31769.
- Capaldi, R. A. and Schulenberg, B. (2000). *Biochim. Biophys. Acta* **1458**, 263–269.
- Capaldi, R. A., Aggeler, R., Wilkens, S., and Grüber, G. (1996). *J. Bioenerg. Biomembr.* **28**, 397–401.
- Cherepanov, D. A., Mulkidjanian, A. Y., and Junge, W. (1999). *FEBS Lett.* **449**, 1–6.
- Cross, R. L. (2000). *Biochim. Biophys. Acta* **1458**, 270–275.
- Cross, R. L., Grubmeyer, C., and Penefsky, H. S. (1982). *J. Biol. Chem.* **257**, 12101–12105.
- Eckstein, F. (1983). *Angew. Chem.* **22**, 423–506.
- Fisher, A. J., Smith, C. A., Thoden, J. B., Smith, R., Sutoh, K., Holden, H. M., and Rayment, I. (1995). *Biochemistry* **34**, 8960–8972.
- Fischer, S., Grüber, P., and Turina, P. (2000). *J. Biol. Chem.* **275**, 30157–30162.
- Fromme, P. and Grüber, P. (1989). *FEBS Lett.* **259**, 33–36.
- Garcia, J. J. and Capaldi, R. A. (1998). *J. Biol. Chem.* **273**, 15940–15945.
- Grüber, P. and Labahn, A. (1992). *J. Bioenerg. Biomembr.* **24**, 493–497.
- Grubmeyer, C., Cross, R. C., and Penefsky, H. S. (1982). *J. Biol. Chem.* **257**, 12092–12100.
- Hausrath, A. C., Grüber, G., Matthews, B. W., and Capaldi, R. A. (1999). *Proc. Natl. Acad. Sci. USA* **96**, 13697–13702.
- Kato-Yamada, Y., Noji, H., Yasuda, R., Kinoshita, K. Jr., and Yoshida, M. (1998). *J. Biol. Chem.* **273**, 19375–19377.
- Jencks, W. P. (1980). *Adv. Enzymol. Related Areas Mol. Biol.* **51**, 75–106.
- Matsuno-Yagi, A. and Hatefi, Y. (1993). *J. Biol. Chem.* **268**, 1539–1545.
- Mendel-Hartvig, J. and Capaldi, R. A. (1991). *Biochemistry* **30**, 10987–10991.
- Nalin, C. M. and Cross, R. L. (1982). *J. Biol. Chem.* **257**, 8055–8060.
- Noji, H., Yasuda, R., Yoshida, M., and Kinoshita, K., Jr. (1997). *Nature (London)* **386**, 299–302.
- Oster, G. and Wang, H. (2000). *Biochim. Biophys. Acta* **1458**, 482–510.
- Pänke, O., Gumbiowski, K., Junge, W., and Engelbrecht, S. (2000). *FEBS Lett.* **472**, 34–38.
- Penefsky, H. S. (1985a). *J. Biol. Chem.* **260**, 13735–13741.
- Penefsky, H. S. (1985b). *Proc. Natl. Acad. Sci. USA* **82**, 1589–1593.
- Possmayer, F. E., Hartog, A. F., Berden, J. A., and Grüber, P. (2000). *Biochim. Biophys. Acta* **1456**, 77–98.
- Rastogi, V. K. and Girvin, M. E. (1999). *Nature (London)* **402**, 263–268.
- Richter, M. L. and Gao, F. (1996). *J. Bioenerg. Biomembr.* **28**, 443–449.
- Sambongi, Y., Iko, Y., Tanabe, M., Omote, H., Iwamoto-Kihara, A., Ueda, I., Yanagida, T., Wada, Y., and Futai, M. (1999). *Science* **286**, 1722–1724.
- Smith, C. A. and Rayment, I. (1996). *Biochemistry* **35**, 5404–5417.
- Tsunoda, S. P., Muneyuki, E., Amano, T., Yoshida, M., and Noji, H. (1999). *J. Biol. Chem.* **274**, 5701–5706.
- Tsunoda, S. P., Aggeler, R., Noji, H., Kinoshita, K., Jr., Yoshida, M., and Capaldi, R. A. (2000). *FEBS Lett.* **470**, 244–248.
- Turina, P. and Capaldi, R. A. (1994a). *J. Biol. Chem.* **269**, 13465–13471.
- Turina, P. and Capaldi, R. A. (1994b). *Biochemistry* **33**, 14275–14280.
- Wilkens, S. and Capaldi, R. A. (1994). *Biol. Chem. Hoppe Seyler* **375**, 43–51.
- Zhang, S. and Jagendorf, A. T. (1995). *J. Biol. Chem.* **270**, 6607–6614.
- Zhou, J. M. and Boyer, P. D. (1993). *J. Biol. Chem.* **268**, 1531–1538.